Focal loss of the glutamate transporter EAAT2 in a transgenic rat model of SOD1 mutant-mediated amyotrophic lateral sclerosis (ALS)

David S. Howland*†, Jian Liu‡, Yijin She*, Beth Goad*, Nicholas J. Maragakis§, Benjamin Kim§, Jamie Erickson*, John Kulik*, Lisa DeVito*, George Psaltis*, Louis J. DeGennaro*, Don W. Cleveland‡, and Jeffrey D. Rothstein§

*Department of Molecular Genetics, Wyeth Research, CN8000, Princeton, NJ 08543; ‡Ludwig Institute for Cancer Research, University of California at San Diego, La Jolla, CA 92093; and §Department of Neurology, Johns Hopkins University School of Medicine, Baltimore, MD 21287

Edited by Thomas Maniatis, Harvard University, Cambridge, MA, and approved December 5, 2001 (received for review October 11, 2001)

Transgenic overexpression of Cu^{+2}/Zn^{+2} superoxide dismutase 1 (SOD1) harboring an amyotrophic lateral sclerosis (ALS)-linked familial genetic mutation (*SOD1*^{G93A}) in a Sprague–Dawley rat results in ALS-like motor neuron disease. Motor neuron disease in these rats depended on high levels of mutant SOD1 expression, increasing from 8-fold over endogenous SOD1 in the spinal cord of young presymptomatic rats to 16-fold in end-stage animals. Disease onset in these rats was early, ≈115 days, and disease progression was very rapid thereafter with affected rats reaching end stage on average within 11 days. Pathological abnormalities included vacuoles initially in the lumbar spinal cord and subsequently in more cervical areas, along with inclusion bodies that stained for SOD1, Hsp70, neurofilaments, and ubiquitin. Vacuolization and gliosis were evident before clinical onset of disease and before motor neuron death in the spinal cord and brainstem. Focal loss of the EAAT2 glutamate transporter in the ventral horn of the spinal cord coincided with gliosis, but appeared before motor neuron/axon degeneration. At end-stage disease, gliosis increased and EAAT2 loss in the ventral horn exceeded 90%, suggesting a role for this protein in the events leading to cell death in ALS. These transgenic rats provide a valuable resource to pursue experimentation and therapeutic development, currently difficult or impossible to perform with existing ALS transgenic mice.

Amyotrophic lateral sclerosis (ALS) is a late-onset neuromuscular disorder characterized by progressive motor dysfunction that leads to paralysis and eventually death. The pathology of the disease results from the death of large motor neurons in the spinal cord and brainstem (1, 2). ALS occurs in both sporadic and familial forms (3). Familial ALS accounts for ≈5–10% of all reported cases. Approximately 15–20% of familial ALS cases has been linked to inheritance in an autosomal dominant fashion of a mutant form of Cu^{+2}/Zn^{+2} superoxide dismutase 1 (SOD1) (4, 5). SOD1 normally functions in the regulation of oxidative stress by conversion of free radical superoxide anions to hydrogen peroxide and molecular oxygen. Over 90 distinct familial SOD1 mutations have been found to date. SOD1 mutations that have been tested in transgenic mice result in ALS-like motor neuron disease (6–8), but SOD1-null mice do not develop motor neuron disease (9). Furthermore, crossing SOD1-null mice with transgenic ALS mice does not alter disease onset or progression (10). Taken together, these results indicate that familial ALS does not result from loss of SOD1 function but rather an unidentified gain of function. There is no consensus as to the mechanism, and theories include alterations in SOD1 folding, oxidative stress from aberrant catalysis (11), or cytoplasmic aggregates (12). New studies also suggest that the disease is not cell autonomous—that nonneuronal cells are necessary for motor neuron degeneration (13, 14, ¶).

Transgenic mouse models expressing mutant forms of SOD1 (15–21) develop neuromuscular disease very similar to human ALS. Age of onset of disease varies as a function of both the type of mutant expressed in mouse and the relative expression levels attained. High expressing SOD1^{G93A} (13-fold above endogenous SOD1) and G37R SOD1 (7–14-fold above endogenous SOD1) transgenic mice contain membrane-bound vacuoles in cell bodies (15, 22) and dendrites (15, 16, 22), which most likely result from degenerating mitochondria. Lower expressing SOD1^{G93A} mice (7-fold above endogenous SOD1) also contain Lewy-body-like cytoplasmic inclusions in the cell bodies of motor neurons (21) containing SOD1, ubiquitin, and phosphorylated neurofilament (23). SOD1^{G85R} transgenic mice expressing mutant SOD1 as little as 20% of endogenous levels also develop neuromuscular disease characterized by loss of large motor neurons in brainstem and in spinal cord (10, 17). No vacuolization has been reported in G85R mice or in similar mice expressing the murine counterpart mutation G86R (18, 24). However, these mice also develop cytoplasmic inclusions that appear in astrocytes and neurons before clinical signs of disease and dramatically increase in abundance with disease progression (10). SOD1^{G85R} mice have also shown to be deficient in the spinal cord astroglial glutamate transporter EAAT2 (GLT-1), similar to observations in sporadic ALS (25), suggesting that astroglial dysfunction in ALS may contribute to motor neuron degeneration.

We sought to create a transgenic rat model for ALS by using mutant SOD1 to pursue experimental paradigms currently difficult or impossible to achieve in the smaller transgenic mouse models. Rats provide an advantage in pursuit of therapeutic strategies such as stem cell replacement and are the preferred laboratory animal species for pharmacological manipulations.

Materials and Methods

Generation and Characterization of Transgenic Rats Expressing Human SOD1^{G93A}. A 12-kb *Eco*RI/*Bam*HI restriction fragment of the human *SOD1* gene harboring the G93A mutation was microinjected into Sprague–Dawley rat embryos. Transgenic rats were produced as described (26). Embryos were allowed to develop to term and were analyzed for the presence of the transgene. Tail biopsies from 8-day-old rats were digested in proteinase K and then diluted 1:20 in dH_2O followed by heating at 95°C for 15 min. Two microliters were subjected to PCR by using primers SOD-i3f (5′-GTGGCATCAGCCCTAATCCA-3′) and SOD-E4r (5′-CACCAGTGTGCGGCCAATGA-3′) specific to human *SOD1* to determine the genotypes of founders and offspring.

Taqman quantitative DNA PCR was performed to determine DNA copy number of transgene loci segregating from the multiintegrant founders 26, 46, and 51 to their respective F1

This paper was submitted directly (Track II) to the PNAS office.

Abbreviations: SOD1, superoxide dismutase 1; ALS, amyotrophic lateral sclerosis; EMG, electromyography.

†To whom reprint requests should be addressed. E-mail: howland@war.wyeth.com.

¶Clement, A. M., Roberts, E. A., Goldstein, L. S. & Cleveland, D. W. (2001) *Soc. Neurosci. Abstr.* **27,** no. 580.4.

The publication costs of this article were defrayed in part by page charge payment. This article must therefore be hereby marked "*advertisement*" in accordance with 18 U.S.C. §1734 solely to indicate this fact.

 www.pnas.org/cgi/doi/10.1073/pnas.032539299

Table 1. Multiple transgene integrations in SOD1^{G93A} founders were resolved into individual lines

Line	Subline	dCt	Copy no.	Spinal cord hSOD1/rSOD1	Blood hSOD1/rSOD1	Pathology
26	26L	−3	8	nd	0.4	None
	26H	−6	64	8.6	0.8	~115 days
	26HL	−7	72	10.4	1.1	~102 days
46	46L	−0.5	1–2	0.4	<0.1	None
	46H	−2.5	5–6	2.6	0.2	None
51	51L	−2	4	2.2	0.5	None
	51H	−4	16	5.8	1.2	None
61	—	−2.3	4–5	2.4	0.1	None

ND, not determined; H, high copy; L, low copy; h, human; r, rat; dCt, delta cycle threshold.

generation progeny. Primer-probe sets specific for human *SOD1* and an internal normalizer gene, *Thy1.2*, were used in multiplex PCR on a Taqman 770 PCR thermocycler (PE Biosystems) following the manufacturer's recommended conditions. Data were represented as delta cycle threshold (dCt) and were converted to relative transgene DNA copy number by the equation $2^{(-dCt)}$ (Table 1).

Quantitation of SOD1 in Blood and SOD1 and EAAT2 in Spinal Cord. Blood samples from tail vein bleeds were solubilized in 10 vol of 50 mM Tris·HCl, pH 7.5/150 mM NaCl/5 mM EDTA/1% Nonidet P-40/1% SDS. For SOD1 detection, 25 μg was electrophoresed on 12% SDS/polyacrylamide gel and transferred to nitrocellulose. Cervical spinal cord was homogenized in 2 ml of 50 mM Tris·HCl, pH 7.5/150 mM NaCl/5 mM Na_2EDTA/1% Nonidet P-40/1% SDS, and 5 μg was electrophoresed as described above. For detection of EAAT2, ventral horn of cervical spinal cord was dissected by using 0.5-mm micropunches (Zivic–Miller) and homogenized as described above, and 25 μg of total protein was electrophoresed on 7.5% SDS/polyacrylamide gels. Western blots were probed with either anti-SOD1 (27) (1:5,000), anti-GLT-1 (EAAT2; 1:1,000; Chemicon), or anti-actin (C4; 1:10,000; Roche Molecular Biochemicals) Abs.

Immunohistochemical Analyses. Animals were killed by using approved animal welfare protocols and perfused by cardiac puncture with 4% paraformaldehyde/PBS. Muscle, brain, and spinal cord were removed followed by regional dissection of spinal cord and spinal nerve roots. Tissue blocks were embedded in paraffin or araldite for sectioning (7 and 1 μm, respectively). Immunostains and semithin plastic sections were processed as described (16, 17, 28). Hematoxylin and eosin stains of muscle and spinal cord were performed on paraffin sections, whereas semithin sections of spinal roots were stained with toluidine blue. Immunostaining was performed with Abs to neurofilament with SMI-32 (1:8,000; Sternberger–Mayer, Jarrettsville, MD), glutamate transporter GLT-1 (1:1,000), SOD1 (1:10,000), heat shock protein (HSP70; 1:100; StressGen Biotechnologies, Victoria, BC, Canada); ubiquitin (1:1,500; Dako), and glial fibrillary acidic protein (1:50; Dako).

Electrophysiological Recording. Electromyography (EMG) and nerve conductions were performed by using an ADI (Greenwich, CT) Powerlab/8SP stimulator and BioAMP amplifier followed by computer assisted data analysis (CHART 4.0 and SCOPE 3.5.6; ADI). Compound muscle action potentials were recorded by stimulating the sciatic nerve at the sciatic notch and recording from the foot. EMG was performed by using a bipolar needle and sampling at 200 Hz.

Results

Multiple Transgenic Rat Lines Express Mutant SOD1^{G93A}. We identified three SOD1^{G93A} founders that expressed mutant human SOD1 in blood (Fig. 1*A*). A fourth (founder 46) showed no detectable SOD1^{G93A} expression; however, subsequent immunoblots of whole blood from the F1 animals of this line did indeed show low-level SOD1^{G93A} (not shown). These four founders were bred to the F1 generation to establish transgenic lines.

Transgene transmission frequency to the F1 generation was greater than the expected 50% in lines 26, 46, and 51 and was determined to be the result of multiple transgene integration sites in each of these founders. Distinct transgene integrations can be resolved by using quantitative Taqman PCR if the number of transgene copies differs at each chromosomal site. This was indeed the case for lines 26, 46, and 51. Taqman PCR data were used to track inheritance of distinct low- or high-copy transgene loci by F1 generation animals thereby allowing us to establish separate sublineages for each of these lines (Table 1).

Development of Motor Neuron Disease in SOD1^{G93A} Transgenic Rats. SOD1^{G93A} founder 26 developed motor neuron disease at 93 days of age, whereas all other founders did not develop disease. Because of the multiple integration of the transgene, the F1 generation animals derived from founder 26 inherited either the high- or low-copy transgene locus or both (see Table 1). F1 animals containing only the low-copy locus (L26L) did not develop motor neuron disease. F1 animals that inherited both loci from founder 26 (L26HL) developed motor neuron disease by 93 days of age, the same age as disease onset in the founder. F1 animals that inherited only the high-copy locus (L26H) developed motor neuron disease between 104–121 days of age. The apparent earlier onset in L26HL vs. L26H animals most likely was the result of slightly higher mutant SOD1 expression (Table 1). Because the single high-copy locus (L26H) in rats was sufficient to elicit motor neuron disease, we chose to breed this subline to the F2 and subsequent generations for further analysis.

Mutant SOD1 Expression in SOD1^{G93A} Transgenic Rats. SOD1^{G93A} expression in the spinal cord of L26H transgenic rats was determined to be ≈8-fold above endogenous SOD1 as assessed by immunoblot analysis of young presymptomatic animals (Fig. 1*C*; Table 1). As expected, these levels exceeded other transgenic rat lines that did not go on to develop motor neuron disease (Table 1). SOD1^{G93A} expression in L26H rats was also evident across many brain regions as well as peripheral tissues (Fig. 1*B*), similar to that seen in described SOD1 transgenic mice (16). By end stage, mutant SOD1 levels accumulated ≈16-fold over endogenous, representing a further 2-fold increase in SOD1^{G93A} compared with levels in young presymptomatic rats (6 weeks old) (Fig. 1*C*). Spinal cord SOD1^{G93A} levels were directly compared

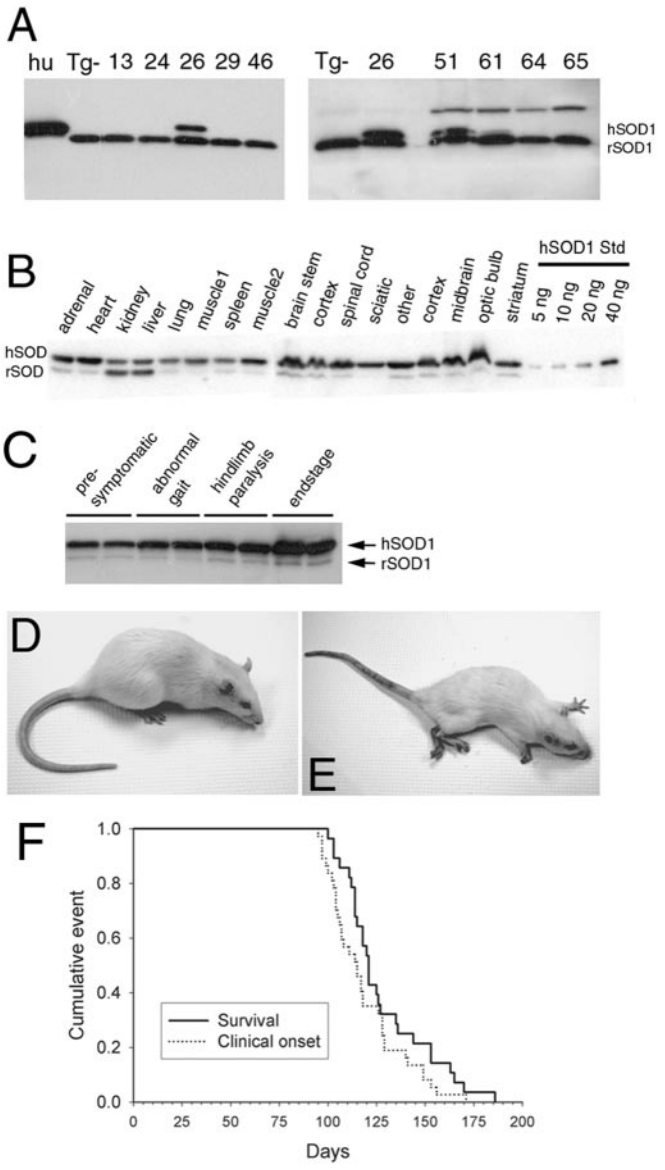

Fig. 1. Mutant SOD1 expression and disease in SOD1^{G93A} transgenic rats. SOD1 expression in blood from transgenic founders (*A*) is highest in founder number 26. L26H F1 generation rats exhibit SOD1^{G93A} expression throughout the nervous system and peripheral tissues (*B*). SOD1^{G93A} expressed at ≈8-fold over endogenous in young (6 weeks) presymptomatic transgenic rat spinal cord increases to ≈16-fold by end-stage disease (16 weeks) (*C*). Normal age-matched littermate control animal (*D*) at ≈120 days compared with an end-stage transgenic rat showing signs of muscle wasting, paralysis of both hindlimbs and one forelimb (*E*). Kaplan–Meyer survival curve (n = 25) generated from F2 generation L26H transgenic rats depicting disease onset and survival.

in end-stage L26H transgenic rats and the previously described G1H and G1L transgenic mice, which also express SOD1^{G93A}. We found that SOD1^{G93A} levels in end-stage G1H and G1L (15, 21, 22) transgenic mice were 3- and 1.5-fold, respectively, higher than levels attained in end-stage L26H transgenic rats (data not shown).

Characterization of Motor Neuron Disease in SOD1^{G93A} L26H Transgenic Rats. A subset (n = 25) of F2 generation animals for L26H were observed closely for onset of disease symptoms, as well as progression to death. Onset of motor neuron disease was scored as the first observation of an abnormal gait or evidence of

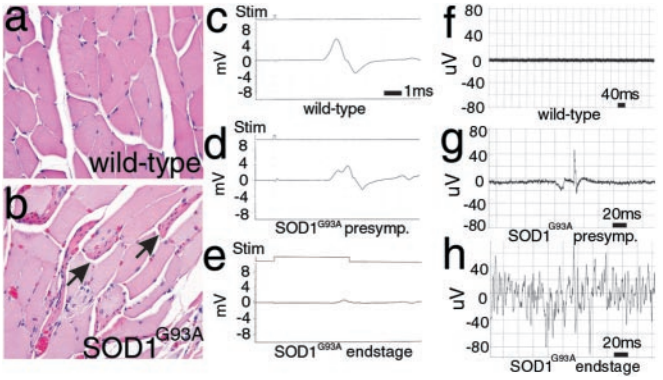

Fig. 2. Muscle atrophy and denervation in SOD1^{G93A} rats. Leg muscle myofibers from end-stage (age >120 days) SOD1^{G93A} rats were often seen as groups of atrophic angular fibers (*b*, arrows), compared with aged-matched control rats (*a*). Compound muscle action potential in nontransgenic control foot muscle (*c*; 5.48 mV) was reduced in the foot (*d*; 4.3 mV) in presymptomatic rats and was almost unobtainable in end-stage foot (*e*; 0.71 mV) after supramaximal stimulation (1 ms per division). Needle EMG of presymptomatic SOD1^{G93A} rat (*g*) demonstrates a rare fibrillation potential recorded in the lumbosacral paraspinous muscles compared with age-matched wild-type control rat (*f*). EMG of end-stage (>125 days age) SOD1^{G93A} rat (*h*) revealed continuous fibrillation potentials and positive sharp waves (20 ms per division).

hindlimb weakness. Affected animals were tested daily for the ability to right themselves after being turned on either side for a maximum of 30 sec; failure at this task was seen in end-stage animals and scored as "death" (see Fig. 1*E*). All end-stage animals were killed. Righting reflex failure was coincident with complete paralysis of both hindlimbs and at least 1 forelimb. F2 L26H transgenic rats had an average age of onset of motor neuron disease of 115 days. Onset typically appeared as hindlimb abnormal gait and progressed very quickly (1–2 days) to overt hindlimb paralysis, typically affecting one limb first. Within 1–2 days, the second hindlimb was involved, although animals could still ambulate through the use of forepaws. Affected rats showed signs of weight loss, poor grooming, and porphyrin staining around the eyes. L26H transgenic rats typically reached end-stage disease very quickly, an average of 11 days after onset of symptoms. All F2 generation L26H transgenic rats monitored for this study reached end-stage disease within 173 days after birth.

Muscle Pathology and Impaired Function in SOD1^{G93A} L26H Rats. Leg muscles (distal and proximal) from end-stage rats revealed obvious and frequent angular atrophic myofibers, most often in discrete clumps typical of neurogenic atrophy (Fig. 2*b*), whereas muscles from wild-type littermate controls were normal (Fig. 2*a*). In parallel, electrophysiologic recordings from end-stage SOD1^{G93A} rats (n = 5) exhibiting obvious hindlimb paralysis or paresis revealed markedly reduced amplitude of compound motor action potentials (CMAP) in the intrinsic foot muscles (Fig. 2*e*), indicating motor neuron loss (compare 5.48 mV in wild-type animals to 0.71 mV in end-stage SOD1^{G93A} rats). CMAP in presymptomatic animals was diminished only partially (Fig. 2*d*; n = 5) compared with littermate controls (Fig. 2*c*). Needle EMG of age-matched wild-type rats demonstrated absence of any spontaneous activity, compared with rare fibrillation potentials in paraspinal muscles from presymptomatic rats (Fig. 2 *f* and *g*). Continuous fibrillation potentials and positive sharp waves were evident in leg muscles from end-stage L26H rats (Fig. 2*h*).

Immunohistochemical Characterization of SOD1^{G93A} L26H Transgenic Rats. Analysis of hematoxylin/eosin-stained sections of lumbar spinal cord from end-stage SOD1^{G93A} rats (n = 10) revealed a

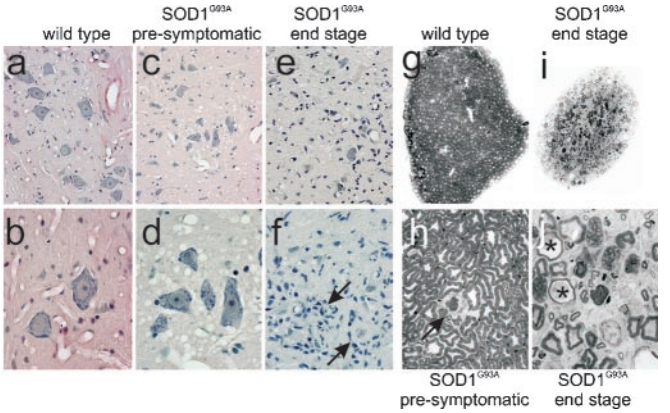

Fig. 3. Motor neuron and axon loss in SOD1^{G93A} rats. Ventral spinal cord gray matter reveals vacuolar degeneration in the neuropil of presymptomatic SOD1^{G93A} rats (*c* and *d*) and astrogliosis and loss of motor neurons in end-stage rats (*e* and *f*) compared with age-matched wild-type rats (*a* and *b*). Glial nodules, around remnants of degenerating motor neurons, were evident throughout the ventral gray matter (*f*, arrows). Ventral motor roots from an end-stage rat (*i*) were atrophic compared with aged-matched control roots (*g*). Closer inspection revealed active ongoing degeneration in end-stage SOD1^{G93A} ventral roots (*j*), whereas roots from presymptomatic rats showed little degeneration (*h*). Magnification: ×4, *g* and *i*; ×10, *a*, *c*, and *e*; ×40, *b*, *d*, and *f*; ×100, *h* and *j*.

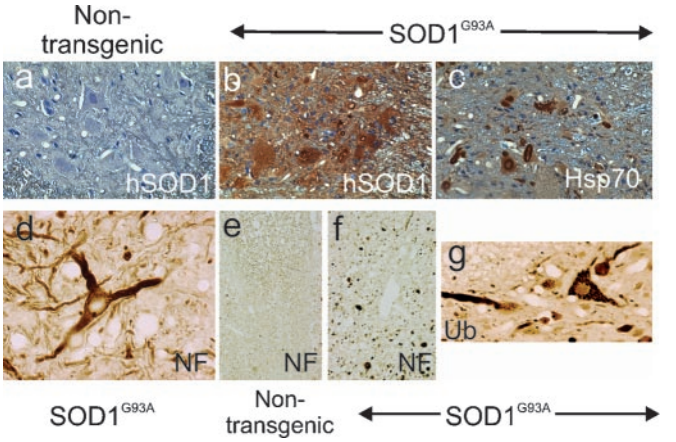

Fig. 4. Aberrant accumulations of proteins in SOD1^{G93A} rats. Accumulation in the neuropil of SOD1^{G93A} rats (*b*) compared with age-matched wild-type rats (*a*). Hsc70 (*c*) and ubiquitin (Ub) (*g*) were abnormally accumulated in the neuropil and cytoplasm of ventral gray neurons. Similarly, neurofilament (NF) aggregates were found in the soma of large motor neurons (*d*) and their axons, often in spheroid structures in the neuropil and especially in the ventral root zone white matter (*f*) compared with dorsal white tracts (*e*).

dense gliosis with a complete loss of ventral large motor neurons (alpha-motor neurons) as shown in Fig. 3 *e* and *f* compared with similarly aged wild-type rats (Fig. 3 *a* and *b*). Closer inspection demonstrated frequent "glial nodules" (Fig. 3*f*, arrows), representing active degeneration and engulfment of neurons. Inspection of ventral horn gray matter from lumbar spinal cord from presymptomatic rats (≈90–100 days of age) revealed a normal population of motor neurons but a profound vacuolar degeneration of the neuropil (Fig. 3 *c* and *d*), similar to that seen in end-stage SOD1^{G93A} mice (15, 22). However, in the rat these vacuoles were transient, appearing at the time of active motor neuron loss but were nearly absent in the lumbar cord by end-stage disease (Fig. 3 *e* and *f*). Brainstem and cervical spinal cord of end-stage rats also revealed vacuolar and glial nodule changes in motor neurons (not shown), albeit these appeared later in these regions, again consistent with vacuolar presence preceding neuronal loss. In concert with the changes in gray matter, ventral roots from end-stage SOD1^{G93A} rats were atrophic (Fig. 3*i*). On closer inspection (Fig. 3*j*) active degeneration of most axons was observed with macrophage infiltration and myelin ovoids. In contrast, analysis from presymptomatic SOD1^{G93A} rat ventral roots ($n = 5$) showed almost normal-appearing axons (Fig. 3*h*), compared with age-matched controls (Fig. 3*g*), with rare (1–2 axons per root) undergoing degeneration (Fig. 3*h* arrow).

As was reported in earlier examples of SOD1 mutant-mediated disease in mice (10), onset of clinical disease was accompanied by aggregates of SOD1 throughout the rat ventral horn (Fig. 4*b*) and brain (not shown) especially in prominent focal deposits in which mutant SOD1 immunoreactivity was frequently most robust at the perimeter. Similar pathology was not found in nontransgenic controls (Fig. 4*a*). These aggregates could be found in a few surviving motor neuron perikarya, axons, and surrounding glia. Aggregates were intensely stained with Abs to ubiquitin (Fig. 4 *g*), consistent with disruption in protein clearance by the proteosome. Aggregates also contained endogenous Hsc70 especially within surviving motor neuron cell bodies (Fig. 4*c*), suggesting mutant-dependent depletion of the intracellular protein folding chaperone pool. Aberrant accumulations of neurofilaments, reported in SOD1^{G93A}-expressing transgenic mice (29), were prominent abnormalities after disease onset, both in perikarya (Fig. 4*d*) and in distended axonal swellings [compare the neurofilament staining in transgenic axons (Fig. 4*f*) with that of the wild-type littermate controls (Fig. 4*e*)]. These accumulations were selective for axons within the ventral root exit zone and were not found in the dorsal ascending columns (not shown).

EAAT2 Deficits in the Ventral Horn Spinal Cord of SOD1^{G93A} L26H Rats. EAAT2 is the predominant glutamate transporter in the central nervous system, normally expressed widely throughout the spinal gray matter (Fig. 5*a*) in astrocytes but not in motor neurons (arrows, Fig. 5*b*). Previous studies have documented a profound loss of the protein in sporadic and familial ALS (25, 28, 30). In presymptomatic SOD1^{G93A} rats, just before disease onset, motor neurons are still present (Fig. 5*c*, arrows) and ventral horns have not started to degenerate (Fig. 3*h*). At this time point, there is an obvious patchy loss of EAAT2 immunoreactivity in the ventral horn (Fig. 5*c*). By end stage, there is a profound focal loss of EAAT2 immunoreactivity despite a striking increase in the number of astrocytes (Fig. 5 *d* and *e*). These changes were mirrored by a quantitative loss of EAAT2 immunoreactivity measured from immunoblots of extracts from spinal cord, especially in the ventral gray regions (Fig. 5*f*). Assays of glutamate transport also confirmed a nearly 50% loss of functional transport (data not shown). Astroglial reactivity, as revealed by glial fibrillary acidic protein immunostaining, also showed activation before motor neuron degeneration, in presymptomatic spinal cord ventral gray (Fig. 5*h*) compared with nontransgenic controls (Fig. 5*g*), followed by a more dramatic activation (Fig. 5 *i* and *j*) in end-stage tissue.

Discussion

We have generated transgenic Sprague–Dawley rats that express human mutant SOD1^{G93A} at levels ≈8-fold over endogenous SOD1 in the spinal cord of young presymptomatic rats. This level of expression was sufficient to cause an ALS-like motor neuron disease in rats by 3–4 months of age. Additional transgenic lines expressing mutant SOD1 between 0.1- to ≈6-fold over endogenous levels of SOD1 have not developed any signs of motor neuron disease by 1 year of age. Recapitulation of an ALS-like motor neuron disease in the transgenic rat using the G93A

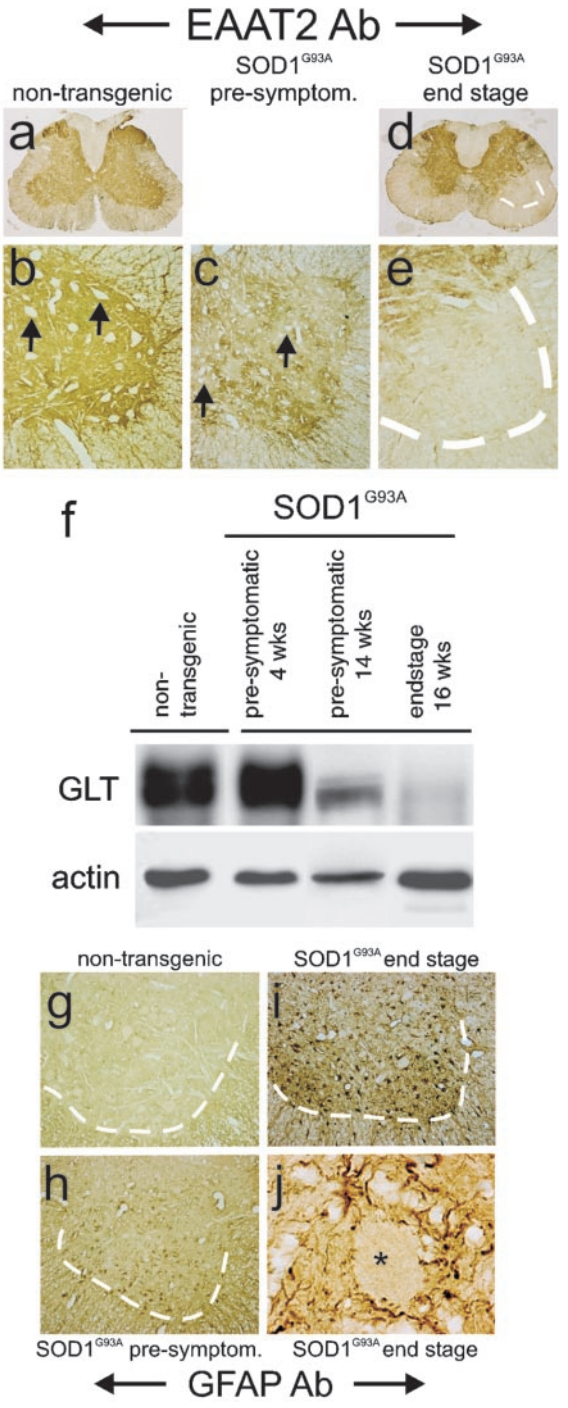

Fig. 5. Astroglial alterations in SOD1^{G93A} rats. The usual ubiquitous astroglial expression of the glutamate transporter EAAT2 (*a* and *b*), surrounding motor neurons (arrows), was markedly altered in SOD1^{G93A} rats with a patchy loss in the ventral horn in presymptomatic rats (*c*) and almost a complete loss of protein in end-stage ventral gray from SOD1^{G93A} rats (*d* and *e*). This loss of EAAT2 (GLT) was paralleled in immunoblots from ventral gray of presymptomatic and end-stage rats (*f*). In parallel, astroglial expression of glial fibrillary acidic protein (GFAP) increased somewhat in presymptomatic ventral gray (*h*), compared with age-matched wild-type control (*g*), and was markedly increased in end-stage rats (*i*), especially around rare motor neuron profiles (*j*).

mutant SOD1 clearly depended on the ability to obtain high-level transgene expression in the spinal cord as reported for the SOD1^{G93A} (15) and SOD1^{G37R} (16) transgenic mice.

No overt motor neuron loss was evident in presymptomatic SOD1^{G93A} transgenic rats between 3–4 months of age as determined by both histological and electrophysiological observations. However, we noted the appearance of vacuoles in motor neurons as well as gliosis preceding both motor neuron loss and clinical signs of disease in rats. The presence of vacuoles was transient, correlating with the time of active motor neuron loss. In the most affected regions vacuoles were nearly absent by end-stage disease. Progression to end-stage paralysis was rapid, with an average of 11 days after first observation of symptoms. This finding is in contrast to the slower progression of disease observed in SOD1^{G93A} transgenic mice (G1H and G1L) where disease duration approached 60–70 days (15, 21, 22) but instead was more similar to that reported for SOD1^{G85R} mice (17) whose disease duration was only 7–14 days. Mutant SOD1 levels in end-stage G1L and G1H transgenic mouse spinal cord (15, 21, 22) were higher than in SOD1^{G93A} L26H transgenic rats, and therefore the rapid progression of disease in the SOD1^{G93A} transgenic rats seems not to be a function of expression levels but rather may be characteristic of a species difference in the presentation of clinical phenotype. The rapid decline of the SOD1^{G93A} rats coincided with substantial loss of spinal cord motor neurons as well as marked increases in gliosis and degeneration of muscle integrity and function.

The astroglial glutamate transporter EAAT2 is the primary means of maintaining low extracellular glutamate levels. Loss of this protein induced by either pharmacological or molecular methods *in vitro* and *in vivo* results in increased extracellular glutamate, as measured by microdialysis and excitotoxic neuronal degeneration, including degeneration of motor neurons. Elevations of extracellular glutamate and loss of EAAT2 are characteristic of at least 40% of sporadic patients with ALS, and similar changes have been observed in the mutant mouse models of the disease (17, 25, 31–33). Interestingly, a recent study of a similar transgenic rat model, however, did not observe changes in cerebrospinal fluid (CSF) glutamate (34). The reason for the difference between that rat model, the work in the current study, and previous human observations is not clear. However, a focal loss of EAAT2 would be expected to increase glutamate only locally and therefore might not be detectable in the CSF. In addition, CSF glutamate measurements are fraught with technical problems.

The cause of EAAT2 loss is not known, but multiple studies demonstrate that astroglial changes can occur early, before actual motor neuron degeneration (13, 17). However, loss of neurons can lead to glial responses that include transient down-regulation of EAAT2 expression (35, 36). Yet, there is no loss of EAAT2 in another motor neuron disease, spinal muscular atrophy (33, 37). Previous reports have documented a loss of EAAT2 to ≈50% its normal level in SOD1^{G85R} transgenic mice (17) by using whole spinal cord at end-stage disease. The current study provides a thorough evaluation of EAAT2 at a time point when motor neurons are intact histologically and physiologically, as revealed by EMG/nerve conduction studies. At these "early" time points, there was a patchy loss of EAAT2 expression around motor neurons in the ventral gray areas of the spinal cord, suggesting that the loss of EAAT2 may contribute to motor neuron degeneration. Concomitant with decreased EAAT2 expression was a marked increase in gliosis, and by end stage, where motor neuron loss is severe, EAAT2 was present at only 5–10% of normal levels in the ventral horn. Importantly, the contribution of altered EAAT2 expression to neuronal death/injury was demonstrated by a recent study where EAAT2 overexpression offered protection in SOD1^{G93A} mice.[‖]

[‖]Sutherland, M. L., Martinowich, K. & Rothstein, J. D. (2001) *Soc. Neurosci. Abstr.* **27,** no. 607.6.

We describe a transgenic rat model for ALS based on the *SOD1*^{G93A} mutation. The clinical and pathological changes displayed resemble the "high expressing" SOD1^{G93A} mice first described by Gurney *et al.* (15) including a characteristic vacuolar degeneration of the neuropil, which seems to occur just before motor neuron degeneration and aggregates staining with SOD1 and neurofilament. Proteins, Hsc70 and ubiquitin, involved in protein folding as well as degradation are also present in these aggregates in these transgenic rats. Notable differences between the rat and mouse models, however, include a more rapid progression of disease and the transient appearance of vacuoles in the transgenic rat. The rapid decline of the SOD1^{G93A} rats to end stage could account for the disappearance of vacuoles in sections of the spinal cord that display severe motor neuron loss.

We have also demonstrated, using the SOD1^{G93A} rats, that EAAT2 levels decrease in the spinal cord before clinical onset of symptoms and that decrease becomes more severe by end-stage sickness, suggesting a role for glutamate toxicity and astroglial dysfunction in disease pathogenesis.

D.S.H. thanks Drs. Lucie Bruijn, John Moyer, Seung Kwak, and Erika Holzbaur for critical comments and advice. D.W.C. and J.D.R. gratefully acknowledge support from National Institutes of Health Grants NS 27036, NS33958, and AG 12992, and the Center for ALS Research. J.L. is the recipient of a fellowship from the Spinal Cord Disease Foundation. D.W.C. receives salary support from the Ludwig Institute for Cancer Research. This work was initiated by the ALS Association as part of its Lou Gehrig Challenge Initiative.

1. Delisile, M. B. & Carpenter, S. (1984) *J. Neurol. Sci.* **63,** 241–250.
2. Banker, B. Q. (1986) in *Myology*, eds. Engel, A. G. & Banker, B. Q. (McGraw–Hill, New York), pp. 2031–2066.
3. Horton, W. A., Eldredge, R. & Brody, J. A. (1976) *Neurology* **26,** 460–665.
4. Rosen, D. R., Siddique, T., Patterson, D., Figlewicz, D. A., Sapp, P., Hentati, A., Donaldson, D., Goto, J., O'Regan, J. P., Deng, H. X., *et al*. (1993) *Nature (London)* **362,** 59–62.
5. Deng, H. X., Hentati, A., Tainer, J. A., Iqbal, Z., Cayabyab, A., Hung, W. Y., Getzoff, E. D., Hu, P., Herzfeldt, B., Roos, R. P., *et al*. (1993) *Science* **261,** 1047–1051.
6. Morrison, B. M., Morrison, J. H. & Gordon, J. W. (1998) *J. Exp. Zool.* **282,** 32–47.
7. Wong, P. C., Rothstein, J. D. & Price, D. L. (1998) *Curr. Opin. Neurobiol.* **8,** 791–799.
8. Shibata, N. (2001) *Neuropathology* **21,** 82–92.
9. Reaume, A. G., Elliot, J. L., Hoffman, E. K., Kowall, N. W., Ferrante, R. J., Siwek, D. F., Wilcox, H. M., Flood, D. G., Beal, M. F., Brown, R. H., *et al.* (1996) *Nat. Genet.* **13,** 43–47.
10. Bruijn, L. I., Houseweart, M. K., Kata, S., Anderson, K. L., Anderson, S. D., Ohama, E., Reaume, A. G., Scott, R. W. & Cleveland, D. W. (1998) *Science* **281,** 1851–1854.
11. Beckman, J. S., Carson, M., Smith, C. D. & Koppenol, W. H. (1993) *Nature (London)* **364,** 584.
12. Johnston, J. A., Dalton, M. J., Gurney, M. E. & Kopito, R. R. (2000*) Proc. Natl. Acad. Sci. USA* **97,** 12571–12576.
13. Gong, Y. H., Parsadanian, A. S., Andreeva, A., Snider, W. D. & Elliott, J. L. (2000) *J. Neurosci.* **20,** 660–665.
14. Pramatarova, A., Laganiere, J., Roussel, J., Brisebois, K. & Rouleau, G. A. (2001) *J. Neurosci.* **21,** 3369–3374.
15. Gurney, M. E., Pu, H., Chiu, A. Y., Dal Canto, M. C., Polchow, C. Y., Alexander, D. D., Caliendo, J., Hentati, A., Kwon, Y. W. & Deng, H. X. (1994) *Science* **264,** 1772–1775.
16. Wong, P. C., Pardo, C. A., Borchelt, D. R., Lee, M. K., Copeland, N. G., Jenkins, N. A., Sisodia, S. S., Cleveland, D. W. & Price, D. L. (1995) *Neuron* **14,** 1105–1116.
17. Bruijn, L. I., Becher, M. W., Lee, M. K., Anderson, K. L., Jenkins, N. A., Copeland, N. G., Sisodia, S. S., Rothstein, J. D., Borchelt, D. R., Price, D. L. & Cleveland, D. W. (1997) *Neuron* **18,** 327–338.
18. Ripps, M. E., Huntley, G. W., Hof, P. R., Morrison, J. H. & Gordon, J. W. (1995) *Proc. Natl. Acad. Sci. USA* **92,** 689–693.
19. Brannstrom, T., Ernhill, K., Jonsson, A., Nilsson, A. & Marklund, S. (2000) *Brain Pathol.* **10,** 775.
20. Friedlander, R., Brown, R., Gagliardini, V., Wang, J. & Yuan, J. (1997) *Nature (London)* **388,** 31.
21. Dal Canto, M. & Gurney, M. (1997) *Acta. Neuropathol.* **93,** 537–550.
22. Dal Canto, M. & Gurney, M. E. (1995) *Brain Res.* **676,** 25–40.
23. Shibata, N., Hirano, A., Kobayashi, M., Dal Canto, M. C., Gurney, M. E., Komori, T., Umahara, T. & Asayama, K. (1998) *Acta Neuropathol.* **95,** 136–142.
24. Morrison, B. M., Janssen, W. G., Gordon, J. W. & Morrison, J. H. (1996) *J. Comp. Neurol.* **373,** 619–631.
25. Rothstein, J. D., Van Kammen, M., Levey, A. I., Martin, L. J. & Kuncl, R. W. (1995) *Ann. Neurol.* **38,** 73–84.
26. Hogan, B. (1983) *Nature (London)* **306,** 313–314.
27. Pardo, C. A., Xu, Z., Borchelt, D. R., Price, D. L., Sisodia, S. S. & Cleveland, D. W. (1995) *Proc. Natl. Acad. Sci. USA* **92,** 954–958.
28. Rothstein, J. D., Martin, L., Levey, A. I., Dykes-Hoberg, M., Jin, L., Wu, D., Nash, N. & Kuncl, R. W. (1994) *Neuron* **13,** 713–725.
29. Tu, P. H., Raju, P., Robinson, K. A., Gurney, M. E., Trojanowski, J. Q. & Lee, V. M. (1996) *Proc. Natl. Acad. Sci. USA* **93,** 3155–3160.
30. Rothstein, J. D., Martin, L. J. & Kuncl, R. W. (1992) *N. Engl. J. Med.* **326,** 1464–1468.
31. Guo, Z., Kindy, M. S., Kruman, I. & Mattson, M. P. (2000) *J. Cereb. Blood Flow Metab.* **20,** 463–468.
32. Pedersen, W. A., Fu, W., Keller, J. N., Markesbery, W. R., Appel, S., Smith, R. G., Karsarskis, E. & Mattson, M. P. (1998) *Ann. Neurol.* **44,** 819–824.
33. Shaw, P. J., Chinnery, R. M. & Ince, P. G. (1994) *Brain Res.* **655,** 195–201.
34. Nagai, M., Aoki, M., Miyoshi, I., Kato, M., Pasinelli, P., Kasai, N., Brown, R. H. & Itoyama, Y. (2001) *J. Neurosci.* **21,** 9246–9254.
35. Ginsberg, S. D., Martin, L. J. & Rothstein, J. D (1995) *J. Neurochem.* **65,** 2800–2803.
36. Ginsberg, S. D., Rothstein, J. D., Price, D. L. & Martin, L. J. (1996) *J. Neurochem.* **67,** 1208–1216.
37. Lin, C. L., Bristol, L. A., Jin, L., Dykes-Hoberg, M., Crawford, T., Clawson, L. & Rothstein, J. D. (1998) *Neuron* **20,** 589–602.